

CSAR Moving Target Detection with Logarithm Background Subtraction Based on Optimal Azimuth Aperture Analysis



Wenjie Shen, Yun Lin, Fei Teng, Yanping Wang, and Wen Hong

Abstract This paper focuses on moving target detection in single-channel circular-SAR (CSAR). The logarithm background subtraction algorithm described in this paper utilizes the overlapped subaperture logarithm image sequence to detect moving targets. It first models the background image with the input image sequence, and then uses the input images to subtract the background image to cancel the clutter. Finally, the moving target can be detected in a subtracted image sequence. However the detection performance depends on the azimuth aperture width (or otherwise the number of input images in one set of image sequence). Thus, the detection performance is analyzed with two measurements: the signal-to-clutter noise ratio (SCNR) improvement and the clutter cancellation ability. Based on the analysis, the proper azimuth aperture width to achieve the best detection performance could be obtained. The algorithm is validated by the GOTCHA-GMTI dataset.

1 Introduction

Ground moving target detection is an important research area in SAR application because of its all-weather capability. Current applications such as battlefield surveillance and city traffic monitoring depend on multichannel techniques such as displaced phase center array (DPCA) [1], space-time adaptive processing (STAP)

W. Shen (✉) · F. Teng · W. Hong

Key Laboratory of Technology in Geo-spatial Information Processing and Application system, Institute of Electronics Chinese Academy of Science (IECAS), University of Chinese Academy of Science (UCAS), Beijing, China

e-mail: whong@mail.ie.ac.cn

Y. Lin · Y. Wang

School of Electronic and Information Engineering, North China University of Technology, Beijing, China

e-mail: ylin@ncut.edu; ypwang@ncut.edu

© Springer Nature Switzerland AG 2019

E. T. Quinto et al. (eds.), *The Proceedings of the International Conference on Sensing and Imaging, 2018*, Lecture Notes in Electrical Engineering 606,

https://doi.org/10.1007/978-3-030-30825-4_7

[2], along-track interferometry (ATI) [3]. Compared with the multichannel system, the single channel system is still an important part of the current system. Thus, research into moving target detection for single-channel systems is essential.

However, the detection capability of single-channel SAR is limited, as pointed out in Chapman et al. [4]. Recent research reveals that the circular geometry may resolve such single-channel SAR detection problems, such as Poisson et al. and Shen et al. [5, 6]. Our team proposed a moving target detection algorithm at the 2017 IGARSS [6]. A modified version is described in this paper. Compared with Shen et al. [6], the algorithm integrates the log-ratio operator to achieve a better clutter cancellation ability. The radiometric adjustment and constant false alarm rate (CFAR) detector are also added to achieve better performance. However, the optimal detection performance depends on the azimuth aperture width, which is used to generate the subaperture image sequence. Previously, the preset azimuth aperture width was mainly acquired by testing. Therefore, in this paper, we present an analysis on acquiring the parameter for achieving optimal detection performance.

The rest of the paper is organized as follows. Section 2 introduces the processing chain of the logarithm background subtraction algorithm. Section 3 consists of the method, whereas Section 4 presents the algorithm performance analysis, which is composed of data and experiment parameters, the signal-to-clutter noise ratio (SCNR) and clutter cancellation analysis, and the optimal detection result.

2 Processing Chain

The subaperture image can be decomposed into a background image (containing clutter) and a foreground image (contain a moving target). The position of the moving target varies in a subaperture image sequence. The algorithm modeled the background image first, rather than simply making the difference between the subaperture images. The first advantage of this step is that it can avoid the target signature being canceled because of the use of the adjacent images performing subtraction. Another advantage is that the target SCNR could be improved by subtraction processing, which is good for moving target detection.

The processing chain is shown in Fig. 1. The algorithm consists of the following parts:

- (1) Segment the full aperture into small arcs of equal length.
- (2) For each arc, using the same image grid to generate an overlap subaperture logarithm image (OSLI) sequence.
- (3) Performing the radiometric adjustment process on each OSLI sequence to remove the antenna pattern.
- (4) Apply a median filter along the azimuth time dimension to the OSLI sequence to obtain the corresponding background image.
- (5) Generating foreground images by using original OSLI subtracts the background image.
- (6) The target is detected on the foreground images by a CFAR detector.

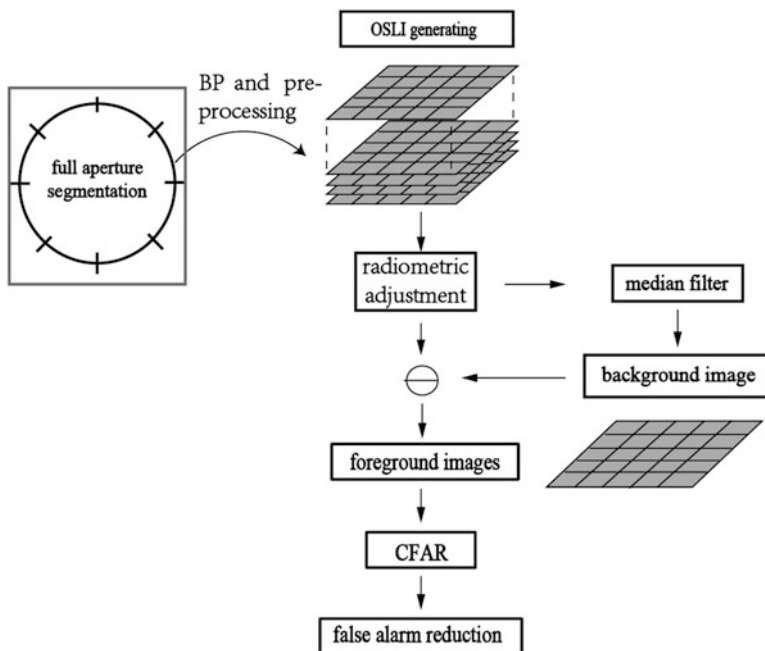


Fig. 1 Processing chain of the logarithm background subtraction algorithm

The moving target detection performance depends on the quality of the modeled background images. The quality of the modeled background images is controlled by the width of the input azimuth aperture (the arc mentioned above, otherwise the number of input images). Thus, in this paper, we mainly discuss the influence of the first step (labeled with a rectangle in Fig. 1) on detection performance.

3 Method

Detecting a moving target requires the SCNR to be high enough; thus, several techniques decrease the clutter energy first such as multichannel techniques. Logarithm background subtraction utilizes such an idea, but the difference is that the background is provided by using the overlapped subaperture image sequence. Thus, the background cancellation result influences the final detection performance. If the width of the input azimuth aperture is too narrow, there may be residual target signature in the background image. If the width of the input azimuth aperture is too wide, the background may mismatch with the clutter in the original image because of its anisotropic behavior. This causes a false alarm. Thus, it is natural to think that there is an optimal width of the input azimuth aperture value so that the target energy is well preserved whereas the clutter is mostly canceled. Two measurements, SCNR

improvement and clutter cancellation quality, are used to find that value. The SCNR improvement factor is used to ensure that the target energy can be much preserved. Clutter cancellation quality is to avoid the defect caused by the anisotropic behavior of the clutter.

We find the proper width of the input azimuth aperture by carrying out the following step. First, we use the clutter cancellation quality data along the width of the input azimuth aperture to find the stable interval during which the clutter value does not vary too much. Then, we find maximum SCNR improvement within the interval. The corresponding angle is the optimal width of the input azimuth aperture.

Therefore, the proper width of the input azimuth aperture should meet the following condition: SCNR improvement reaches its maximum value during interval when the clutter is canceled most.

Improvement of SCNR is shown by the following:

$$G_{\text{SCNR}}(\theta) = 10 \cdot \log \frac{\mu_t(\theta)}{\mu_c(\theta)} - 10 \cdot \log \frac{\mu_{t0}}{\mu_{c0}} \quad (1)$$

$G_{\text{SCNR}}(\theta)$ is SCNR improvement. θ is the width of the input azimuth aperture. μ_{t0} and μ_{c0} are the maximum intensity of the target signature and the reference clutter in the original test frame. $\mu_{t0}(\theta)$ and $\mu_{c0}(\theta)$ are the intensity values extracted from the same position as μ_{t0} and μ_{c0} after subtracting the background generated with different θ . The clutter cancellation ability is evaluated by drawing the curve that $\mu_{c0}(\theta)$ changes along θ .

4 Algorithm Performance Analysis

In this section, we use a selected scene as an example to present the analysis on how to obtain the experiment parameters to achieve the optimal target detection performance with the logarithm background subtraction algorithm. For other CSAR data, the experiment parameter could be acquired by performing the same analysis.

Data and Experiment Parameters

To evaluate the performance, a test frame is selected as shown in Fig. 2. The SAR image is generated with channel one data in GOTCHA GMTI dataset [7]. The aperture width is 0.79° , the center time is 11.2 s. The image grid spacing is $0.2 \text{ m} \times 0.2 \text{ m}$. The target car Durango is delocalized owing to its motion, as labeled with a red rectangle. The reference clutter for SCNR improvement and clutter cancellation ability analysis is labeled with a blue circle.

To study the influence of input azimuth arc size on detection, the 20° azimuth aperture (the test frame is at 0°) is used to generate the overlapped subaperture

Fig. 2 Selected test frame. The target car Durango is delocalized owing to its motion as labeled with a red rectangle. Reference clutter for signal-to-clutter noise ratio (SCNR) improvement and clutter cancellation ability analysis is labeled with a blue circle

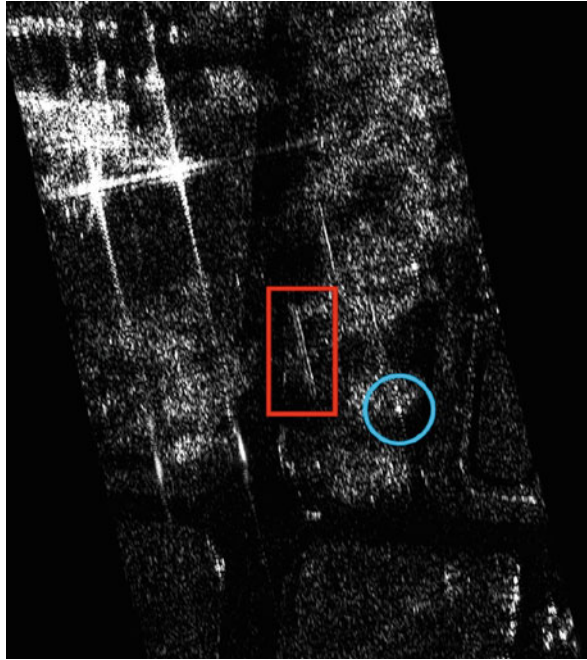


image sequence. Each subaperture image is generated using the same parameters as the test frame. The gap of the azimuth angle between adjacent images is 0.2° . Therefore, we have 100 images for evaluation. To calculate the SCNR, a strong stationary target, which exists within all 20° azimuth apertures, is selected as the reference. The clutter cancellation ability is also evaluated with the strong stationary target. After acquiring the parameter for optimal detection, the example detection result is shown on the test frame.

SCNR Improvement and Clutter Cancellation Analysis

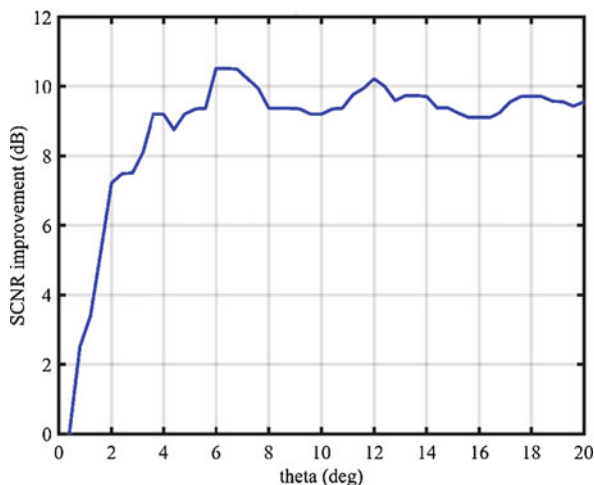
According to the above measurements, we can find the proper θ , which fulfills the above condition as the experiment parameter for optimal detection.

The SCNR improvement curve is shown in Fig. 3.

In Fig. 3, the Durango's SCNR improvement factor increases fast along the θ at $[0^\circ, 6^\circ]$ (the corresponding input images are from 0 to 30) and reaches the peak at 6° . This is because the quality of the background image is improved and the target signature is gradually filtered, as shown in Fig. 4.

In Fig. 4b, the target signature becomes weak but is still visible. In Fig. 4c, the target signature is almost filtered; thus, the improvement is quite high, at around 9 dB. In Fig. 4d, the target signature is fully filtered and has a good improvement

Fig. 3 Signal-to-clutter noise ratio improvement curve



value at 10.52 dB. When $\theta > 6^\circ$, the improvement factor decreases and remains stable at around 9–10 dB. This is because, although the target signature is fully filtered when $\theta > 6^\circ$, the clutter value varies because of its anisotropic scattering behavior. Thus, the causes of the clutter in the test frame cannot be canceled by subtraction processing with model background images.

Take the reference clutter as the example shown in Fig. 5. As mentioned above, the reference clutter could be seen during all 20° . Therefore, we collect the residual clutter value from the same position as in the test frame after subtraction processing to evaluate the clutter cancellation ability. In Fig. 5, the residual clutter values are close to 0 dB during $[0^\circ, 12^\circ]$. This means that its scattering field is stable; therefore, the value is almost equal in the test frame and modeled background image. When $\theta > 12^\circ$, the value is changed because of the anisotropic scattering behavior, thus causing the residual clutter value to gradually increase.

As mentioned previously, the experiment parameter for optimal target detection should fulfill two conditions. Thus, according to the above analysis, the proper width of the input azimuth aperture is $\theta = 6^\circ$ (30 images). In the next section, we present the optimal detection result.

Optimal Moving Target Detection Result

The background image is obtained using 30 overlapped subaperture images. The corresponding background image is shown in Fig. 6.

Compared with test frame shown in Fig. 2, the moving target signatures have been filtered and the clutter structures such as the road edge and building are all preserved. Then, performing the subtraction step, the output image is shown in Fig. 7.

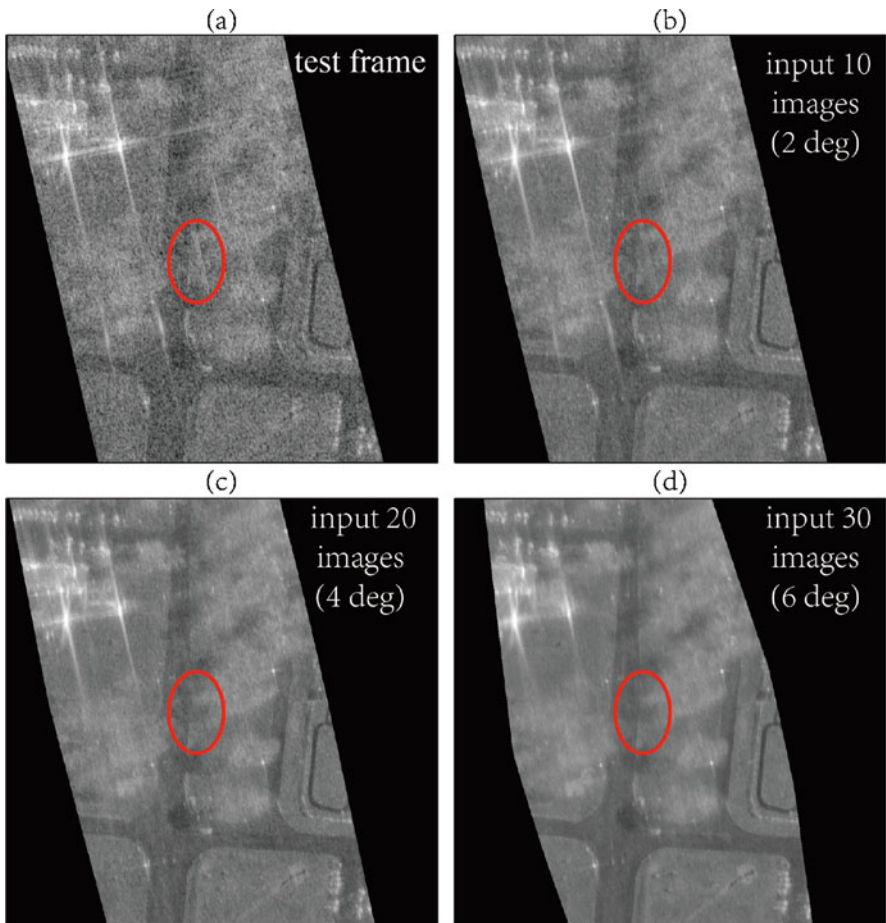


Fig. 4 Test frame and background image modeled with different input image numbers (azimuth aperture width). (a) Test frame. (b–d) Corresponds to the background generated with 10, 20, and 30 input images ($\theta = 2^\circ; 4^\circ; 6^\circ$) respectively. The target signature position is labeled with a red circle

It could be seen in Fig. 7 that the moving target is well preserved. Except for the moving target signatures, the side lobe of the strong stationary target also exists. This is because the side lobe of this stationary target rotates during the 30 input images. Therefore, it is filtered in the background and the target’s sidelobe is preserved in the subtracted image.

Apply a CFAR detector to a subtracted image and post-target discrimination processing to reduce the false alarm; the detection result is shown in Fig. 8. The Durango and the potential moving target are labelled in red. At the top left of the figure, the sidelobe of the two strong manmade structures is also detected. This is

Fig. 5 Residual reference clutter curve

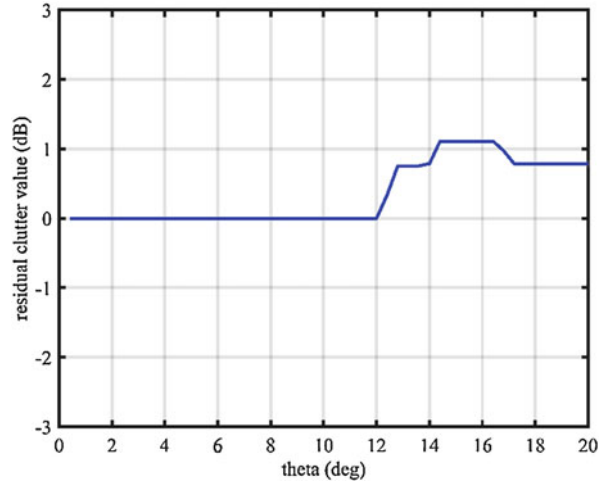
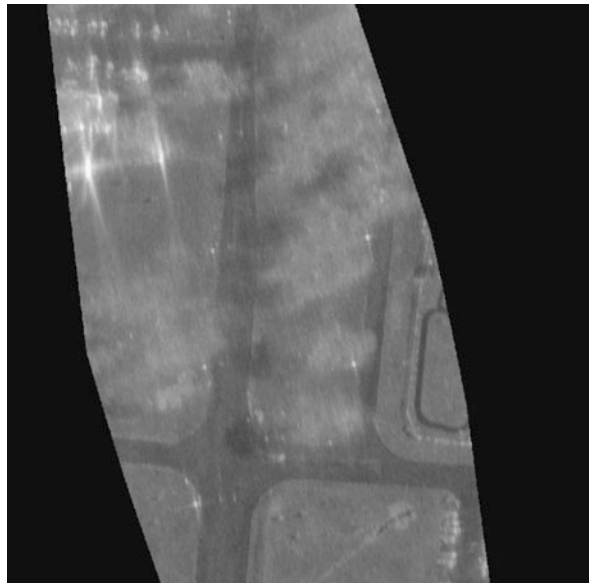


Fig. 6 Modeled background image



because the anisotropic target's rotating sidelobe is not preserved in the background image. It is not canceled; thus, it is falsely detected. The anisotropic behavior-induced false alarm may be excluded by better target discrimination processing in the future.

Fig. 7 Test frame after subtraction processing

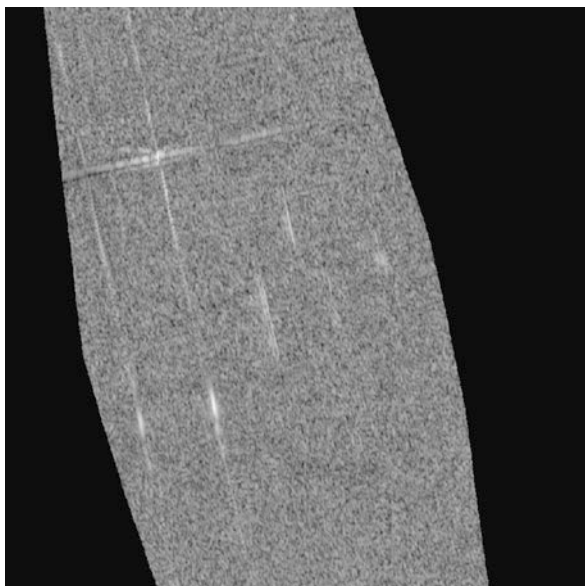
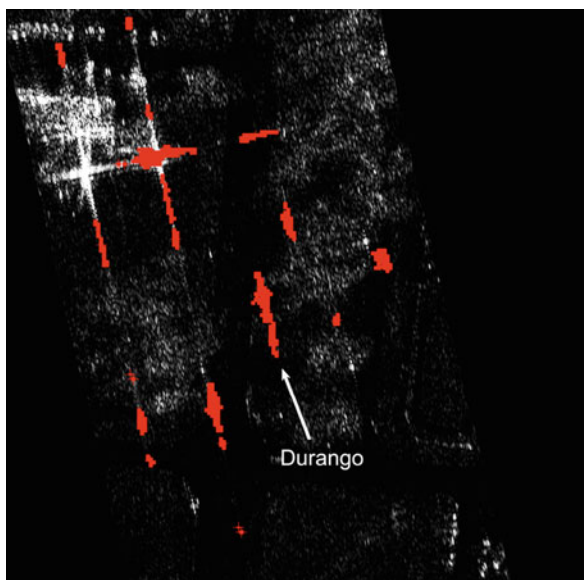


Fig. 8 Detection result



5 Conclusion

In this paper, the performance of the logarithm background subtraction algorithm is evaluated with SCNR improvement and clutter cancellation ability, two measurements. Following the presented analysis, the parameter of the proper number of

input images (or otherwise the width of the input azimuth aperture) for achieving the optimal moving target detection can be determined. Other CSAR data that use the logarithm background subtraction algorithm can follow the same routine. Future work will involve studying better target discrimination processing to reduce the false alarm induced by the anisotropic backscattering behavior of the clutter.

Acknowledgments This work was supported by the Scientific Research Foundation of North China University of Technology, and supported by the Science and Technology Innovation Project of North China University of Technology. This work was also supported by the National Natural Science Foundation of China under Grant 61571421 and Grant 61431018.

References

1. Cerutti-Maori, D., & Sikaneta, I. (2013). A generalization of DPCA processing for multichannel SAR/GMTI radars. *IEEE Transactions on Geoscience and Remote Sensing*, *51*, 560–572.
2. Ender, J. H. G. (1999). Space-time processing for multichannel synthetic aperture radar. *Electronics Communication Engineering Journal*, *11*, 29–38.
3. Chapin, E., & Chen, C. W. (2009). Airborne along-track interferometry for GMTI. *IEEE Aerospace and Electronic Systems Magazine*, *24*, 13–18.
4. Chapman, R. D., Hawes, C. M., & Nord, M. E. (2010). Target motion ambiguities in single-aperture synthetic aperture radar. *IEEE Transactions on Aerospace and Electronic Systems*, *46*, 459–468.
5. Poisson, J. B., Oriot, H. M., & Tupin, F. (2015). Ground moving target trajectory reconstruction in single-channel circular SAR. *IEEE Transactions on Geoscience and Remote Sensing*, *53*, 1976–1984.
6. Shen, W., Lin, Y., Zhao, Y., Yu, L., & Hong, W. (2017). Initial result of single channel CSAR GMTI based on background subtraction. In: *2017 IEEE International Geoscience and Remote Sensing Symposium (IGARSS)*, pp. 976–979.
7. Deming, R., Ilin, R., & Best, M. (2013). Phase-wrapping ambiguity in along-track interferometry. In: *2013 Proc. SPIE*, Bellingham, WA (Vol. 8746, p. 87460E).